NORTHEAST UTILITIES

THE CONNECTICUT LIGHT AND POWER COMPANY
WESTERN MASSACHUSETTS ELECTRIC COMPANY
HOLYOKE WATER POWER COMPANY
NORTHEAST UTILITIES SERVICE COMPANY
NORTHEAST NUCLEAR ENERGY COMPANY

General Offices • Selden Street, Berlin, Connecticut

P.O. BOX 270
HARTFORD, CONNECTICUT 06141-0270
(203) 666-6911

April 9, 1984

Docket No. 50-423
B11118

Director of Nuclear Reactor Regulation
Mr. B. J. Youngblood, Chief
Licensing Branch No. 1
Division of Licensing
U.S. Nuclear Regulatory Commission
Washington, D.C. 20555

Dear Mr. Youngblood:

Millstone Nuclear Power Station, Unit No. 3
Transmittal of Responses to Structural Audit Items

The attached responses are provided to close out Items 8, 14, 15, and 25 from the NRC Structural Audit of February 27 through March 2, 1984.

As discussed with your Mr. Nilesh Chokshi and Mr. David Jeng on April 2, 1984, we will provide responses to all remaining open and confirmatory items on or before May 1, 1984. It was also agreed that Northeast Utilities Service Company will meet with Mr. Chokshi and Mr. Jeng at that time to discuss the information provided in our responses. A date for this meeting will be scheduled later.

If you have any concerns related to the information contained herein or any questions related to our responses, please contact our licensing representative, Ms. C. J. Shaffer at (203) 665-3285.

Very truly yours,

NORTHEAST NUCLEAR ENERGY COMPANY, et al
By Northeast Nuclear Energy Company, Their Agent

W. G. Counsil
Senior Vice President

B001
1/1

STATE OF CONNECTICUT)
) ss. Berlin
COUNTY OF HARTFORD)

Then personally appeared before me W. G. Counsil, who being duly sworn, did state that he is Senior Vice President of Northeast Nuclear Energy Company, a Licensee herein, that he is authorized to execute and file the foregoing information in the name and on behalf of the Licensees herein and that the statements contained in said information are true and correct to the best of his knowledge and belief.

Lorraine J. D'Amico
Notary Public

My Commission Expires March 31, 1988

ITEM 8 Provide justification for not considering cracked sections on containment internals in seismic analysis.

Response:

In the seismic analysis of the containment structure it was assumed that cracked section properties of the internals will not have any significant change in the overall response of the structure. To verify this assumption another calculation was performed using the cracked section properties of one of the steam generator cubicles. The dynamic model utilized considered the containment exterior wall to be cracked.

Figure 8-1 shows the key plan showing the steam generator cubicle for which the cracked section properties were used.

Figure 3.7B-9 shows the dynamic model of the containment structure. In this model members 4, 5, 6, and 7 have stiffness characteristics which are determined from cross sections which include the steam generator cubicle walls. In the verification analysis, members 4, 5, 6, and 7 have been modified to account for cracking of the "B" steam generator cubicle wall.

Conclusion:

Table 8-1 shows the comparison of frequencies of uncracked vs cracked case.

Due to cracking of one steam generator cubicle the shift in the fundamental frequency of the internals is insigifnicant and will have negligible effects on the structural response. Maximum percent shift the frequencies falls well within the peak spreading criteria of ±15 percent. (Ref. FSAR 3.8). Also shown in Table 8-2 is a comparison of resultant accelerations from the cracked versus uncracked sections and the variations were found to be negligible.

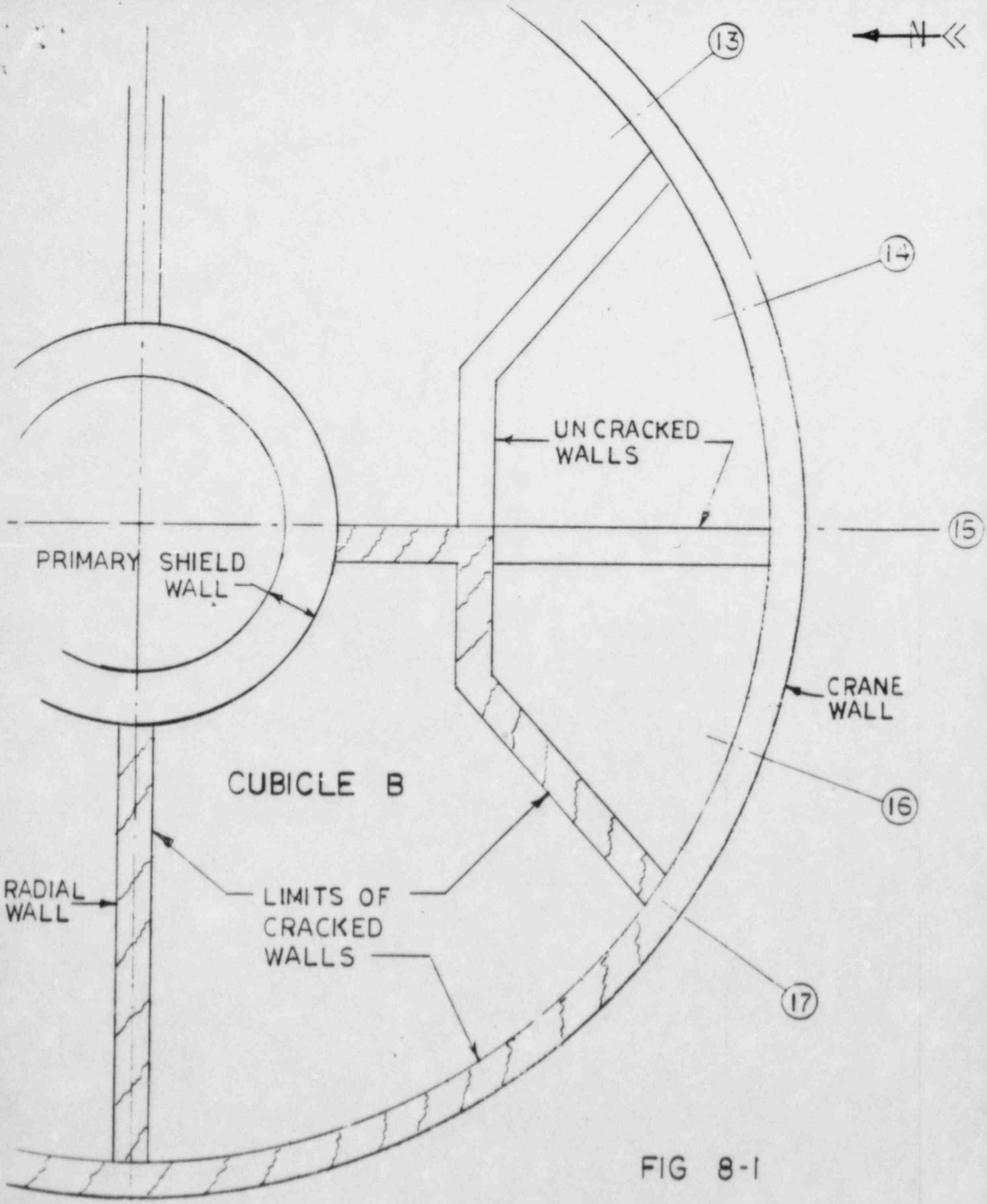

FIG 8-1

PLAN OF ST GEN CUBICLE
SHOWING CRACKED WALLS

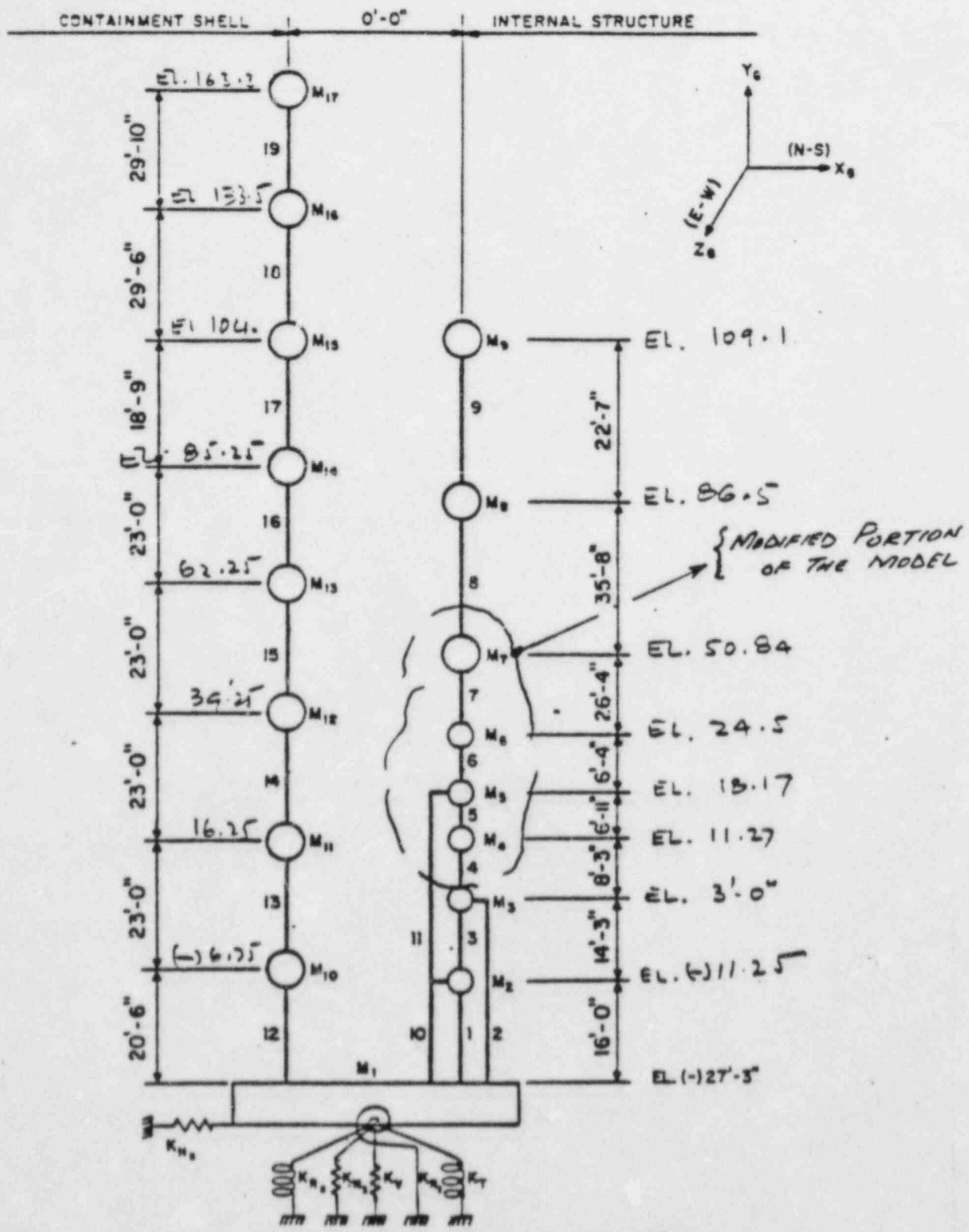

FIGURE 8-2
DYNAMIC MODEL OF
THE CONTAINMENT STRUCTURE
MILLSTONE NUCLEAR POWER STATION
UNIT 3

K_H, K_V, K_R, K_T
HORIZONTAL, VERTICAL, ROCKING AND
TORSIONAL SUBGRADE SPRINGS

TABLE 8-1

	Uncracked Internal		Cracked Internal	
Mode	Eigenvalue	Frequency	Eigenvalue	Frequency
1*	462.7	3.424	462.7	3.423
2*	462.7	3.424	462.7	3.423
3	797.8	4.495	683.1	4.160
4	1027.8	5.102	949.9	4.910
5	1109.4	5.301	1039.4	5.131
6	1358.3	5.866	1358.2	5.865
7	2378.0	7.761	2377.8	7.761
8	2378.0	7.761	2378.0	7.761
9	3466.7	9.371	3466.5	9.371
10	3710.2	9.694	3710.1	9.694
11	4735.1	10.95	4735.1	10.95
12	5611.0	11.92	5278.6	11.56
13	5979.3	12.31	5773.8	12.09
14	7049.6	13.36	7046.6	13.36
15	7053.5	13.37	7051.0	13.36
16	9105.6	15.19	9035.8	15.13
17	9809.4	15.76	9809.2	15.76
18	9810.7	15.76	9810.4	15.76
19	11632.1	17.16	11632.0	17.16

*External Structure

TABLE 8-2

SUMMARY

JOINT	ELEVATION (FT.)	ACCELERATION (g's) 'SSE' N-S UNCRACKED INTERNAL	N-S CRACKED INTERNAL	E-W UNCRACK INTERNAL	E-W CRACK INTERNAL	VERT. UNCRACK INTERNAL	VERT. CRACK INTERNAL
2	(-) 11.25	0.273	0.270	0.257	0.290	0.129	0.136
3	3.00	0.327	0.336	0.356	0.319	0.188	0.182
4	11.30	0.353	0.368	0.348	0.351	0.183	0.175
5	18.20	0.388	0.399	0.403	0.382	0.203	0.196
6	24.50	0.427	0.425	0.428	0.429	0.207	0.202
7	50.84	0.552	0.552	0.563	0.557	0.252	0.257
8	86.50	0.894	0.912	0.854	0.861	0.339	0.361
9	109.10	1.130	1.162	1.042	1.103	0.336	0.351
10	(-) 6.8	0.208	0.195	0.202	0.178	0.126	0.116
11	16.30	0.324	0.283	0.315	0.269	0.168	0.168
12	39.25	0.435	0.370	0.428	0.364	0.216	0.216
13	62.25	0.537	0.460	0.530	0.498	0.264	0.256
14	85.20	0.618	0.527	0.626	0.526	0.293	0.291
15	104.00	0.716	0.614	0.722	0.610	0.322	0.320
16	133.50	0.862	0.738	0.860	0.735	0.375	0.364
17	163.30	1.146	0.971	1.138	0.965	0.418	0.411

ITEM 14 Provide a detailed discussion on how the CM and CR are considered in development of stiffness matrix. A discussion was presented and the issue was resolved. The Applicant will provide this response.

Response:

The information is provided in the response to Item 25.

ITEM 25 Provide a verification example for R1G4 computer program.

Response:

The eccentricity between center of mass and center of rigidity in seismic response analysis of Category I buildings is considered as follows:

An equivalent stiffness matrix is generated to represent the real member (i.e., actual wall section between floors) spanning from center of mass of the lower floor to upper floor, considering both the vertical as well as the horizontal center of rigidity as shown on Figure 1. It is assumed that a rigid link connects the center of mass to the center of rigidity of the real member (i.e., C_V and C_H). A principal global stiffness matrix is then developed, considering bending and shear deformations of the wall section by applying unit displacement and rotations at the center of mass and determining the corresponding stiffness terms that result (see Figure 2). As an example, for a unit displacement in the Xp degree of freedom, the resulting stiffness terms are shown on Figure 2a. Similarly, unit displacements and rotations are applied in the remaining degrees of freedom resulting in the principal globe stiffness matrix as given in Table 1. This resulting matrix is then rotated about the Yp axis (Figure 3) through an angle β between principal axis of the wall section and global axis as defined by the mathematical model (i.e. N-S axis and E-W axis generally define the global axis system of the building model). This resulting matrix is then rotated about the Yg axis and Z' axis as indicated in Figure 4 to obtain the equivalent local stiffness matrix of the real member.

A verification example is provided as follows:

Area properties representative of a typical wall section were arbitrarily selected for input to the verification example (see Pg. 9 and Figure 5). These properties were then input into the computer program R1G4 and the resulting R1G4 local stiffness matrix was obtained. This matrix was then used in a STRUDL model (see Figure 6), where global unit displacements and rotations were applied at Node 2 to determine the global stiffness matrix as shown in Table 2. For comparison purposes, a STRUDL frame model was developed (see Figure 7) using the same area properties for the real member as used in the R1G4 model. Similar displacements and rotations were applied to this model and the resulting global stiffness matrix was obtained as shown in Table 2. A review of this table shows that the resulting matrices are comparatively the same, thus demonstrating the adequacy of the computer program R1G4.

NOTE: The off diagonal terms that appear different are due to round-off error resulting from the transformation of the local stiffness matrix (R1G4) to the global system. The magnitude, however, when compared to the other terms of the stiffness matrix, is essentially zero.

METHOD OF ANALYSIS

The RIG 4 program develops an equivalent stiffness matrix for a system of vertical walls between two rigid floors.

This equivalent member connects the center of mass of each respective floor. The real member is composed of one vertical component, each running through the horizontal and the vertical centers of rigidity.

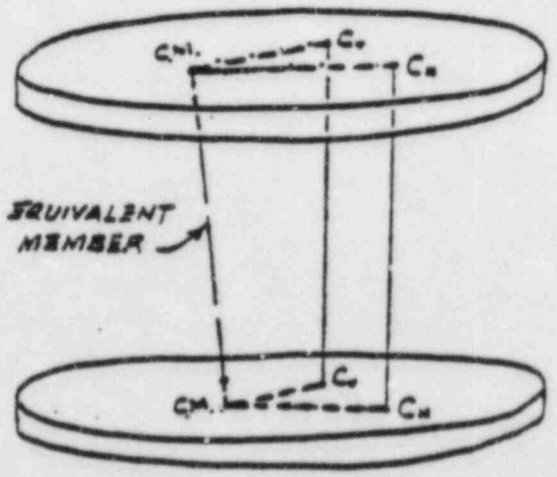

Figure 1 Relationship between a real member and equivalent member

The method involves writing the member stiffness matrix of each individual wall and then rigid body transforming to the local coordinate system of the mass center.

The procedure for these transformations is described on the following pages.

MATHEMATICAL FORMULATION

1. Member stiffness matrix for Principal Global Axes:

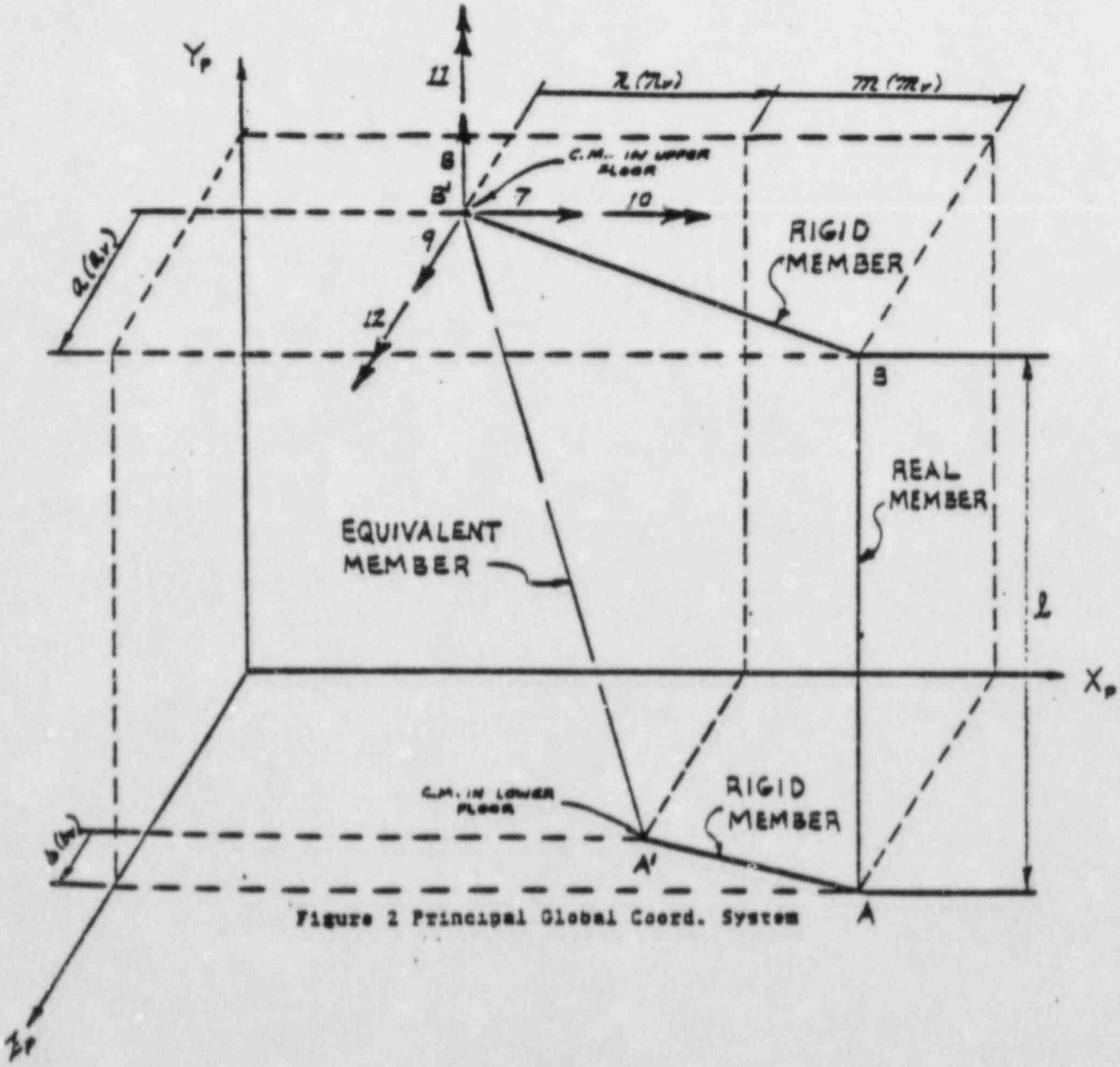

Figure 2 Principal Global Coord. System

Note: The subscript V denotes the vertical center of rigidity

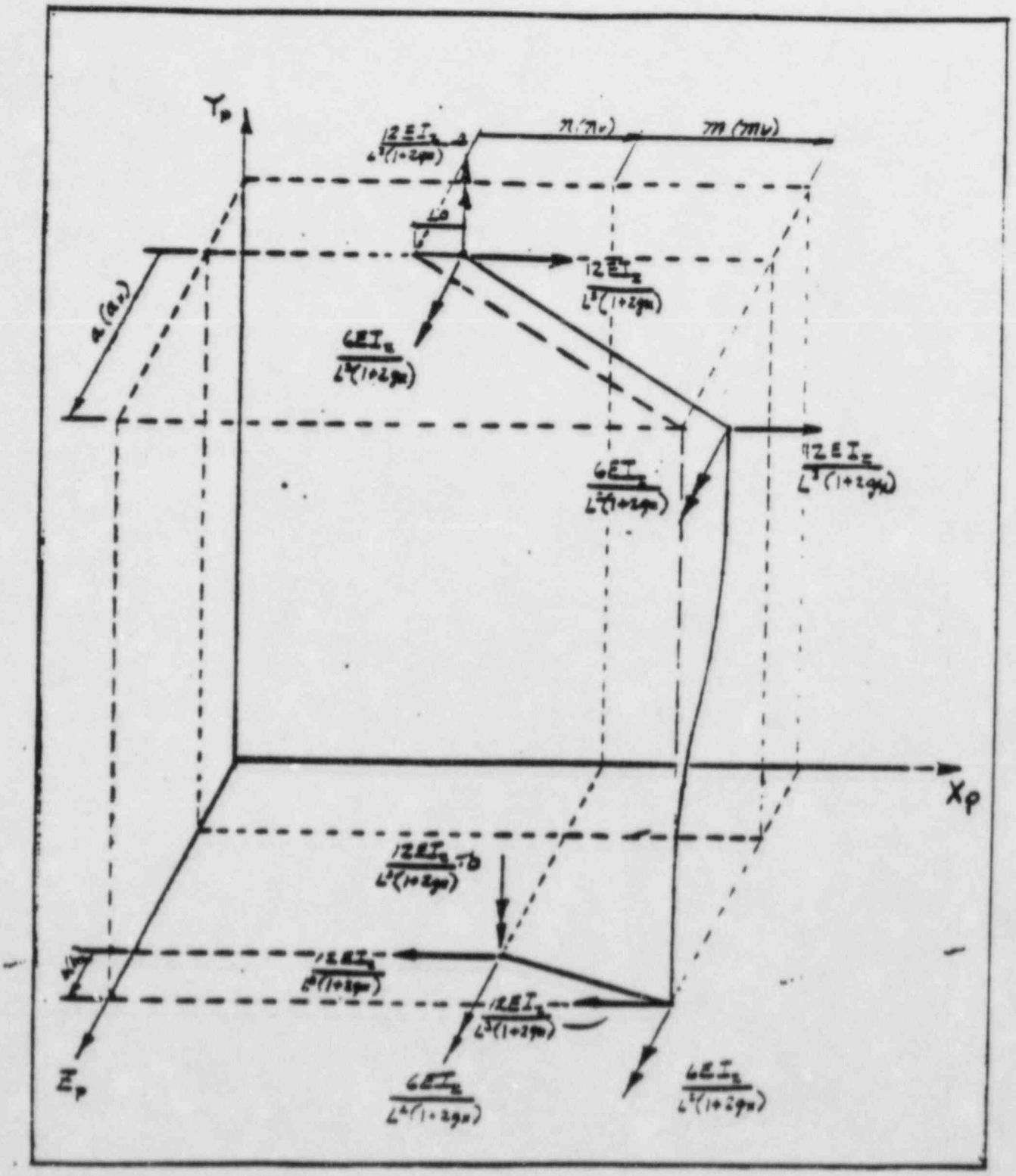
Y_p
X_p
Z_p
$\frac{12EI_z}{L^3(1+2\varphi_z)}$
$\pi_1(\pi_4)$
$\pi_3(\pi_{3V})$
Δ_D
$\frac{12EI_z}{L^3(1+2\varphi_z)}$
$\frac{6EI_z}{L^2(1+2\varphi_z)}$
$\frac{12EI_z}{L^3(1+2\varphi_z)}$
$\frac{6EI_z}{L^2(1+2\varphi_z)}$
$\frac{12EI_z}{L^3(1+2\varphi_z)}$
$\frac{12EI_z}{L^3(1+2\varphi_z)}$
$\frac{12EI_z}{L^3(1+2\varphi_z)}$
$\frac{6EI_z}{L^2(1+2\varphi_z)}$
$\frac{6EI_z}{L^2(1+2\varphi_z)}$

FIGURE 2A

The principal global coordinate system of a structure is defined in Figure 2 in which the member AB is assumed vertical and its principal axes of cross-section are assumed parallel to the principal global axes. Therefore, the stiffness matrix of the equivalent member A'B' in the principal global coordinate system is as shown in Table 1.

Table 1 Member Stiffness Matrix for Principal Global Axes

$$\left[K_{AB}\right]_P = \begin{bmatrix}
\frac{12EI_z}{l^3(1+2g_z)} & & & & \frac{12EI_z}{l^3}\cdot\frac{a}{(1+2g_x)} & \frac{6EI_z}{l^2(1+2g_x)} \\
 & \frac{EA}{l} & & -\frac{EA}{l}\cdot a_y & & \frac{EA}{l}(m+n)_y \\
 & & \frac{12EI_x}{l^3(1+2g_z)} & -\frac{6EI_x}{l^2(1+2g_z)} & -\frac{12EI_x}{l^3}\cdot\frac{(m+n)}{(1+2g_z)} & \\
 & & & \frac{4EI_x(1+0.5g_z)}{l(1+2g_z)} + \frac{EA}{l}a_y^2 & \frac{6EI_x}{l^2}\frac{(m+n)}{(1+2g_z)} & -\frac{EA}{l}(m+n)_y a_y \\
 & & & & \frac{GI_y}{l} + \frac{12EI_z a^2}{l^3(1+2g_x)} + \frac{12EI_x}{l^4}\frac{(m+n)^2}{(1+2g_z)} & \frac{6EI_z}{l^2}\frac{a}{(1+2g_x)} \\
\text{Sym} & & & & & \frac{4EI_z}{l}\frac{1+0.5g_y}{1+2g_x} + \frac{EA}{l}(m+n)_y^2
\end{bmatrix} \quad (1)$$

in which the shear constant:

$$g_z = \frac{6EI_z}{GA_x l^2}$$

$$g_z = \frac{6EI_x}{GA_z l^2}$$

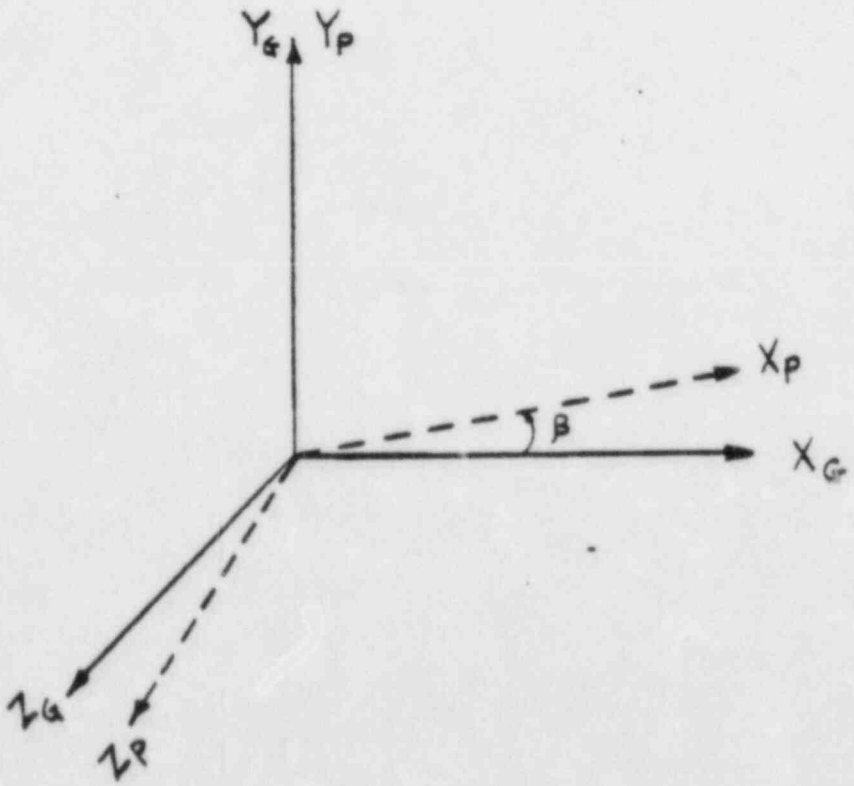

FIGURE 3

The second step in the transformation is the rotation through an angle α about the Y_G axis. This rotation places the X axis in the position denoted as X', which is the intersection of the X_G-Z_G plane and the X_L-Y_G plane. Also, this rotation places the Z_L axis in its final position at the angle α with the Z_G axis (See Figure 4). The last step in transformation consists of the rotation through an angle γ about the Z_L axis. This rotation places the X_L and Y_L axes in their final positions, as shown in Figure 4.

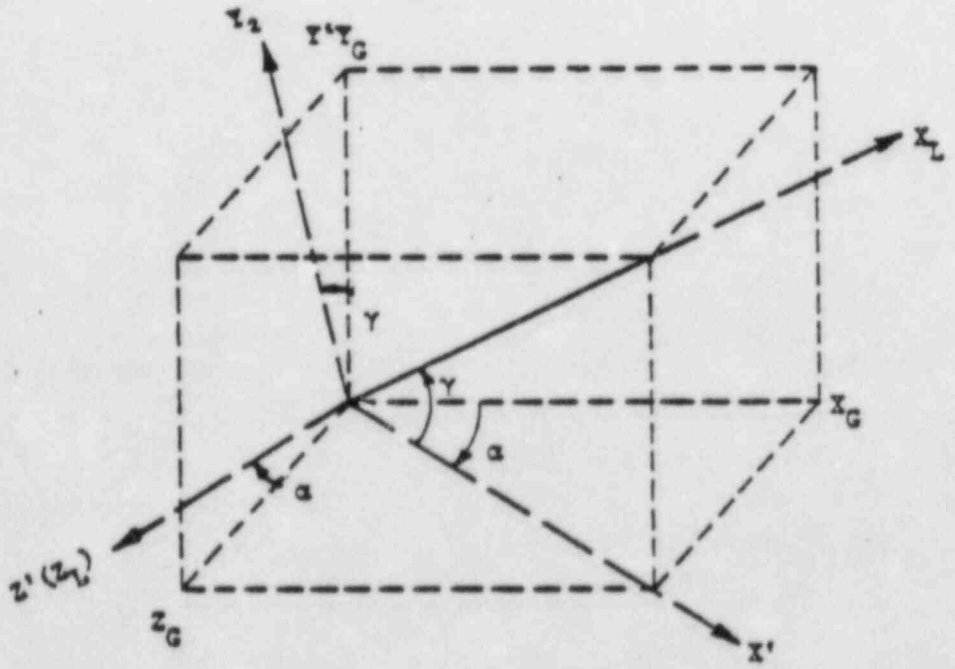

Figure 4 Rotation of axes for a space member

FIGURE 5

RELATIONSHIP BETWEEN LOCAL MEMBER (REAL) PRINCIPAL, PRINCIPAL GLOBAL* AND GLOBAL AXIS SYSTEM

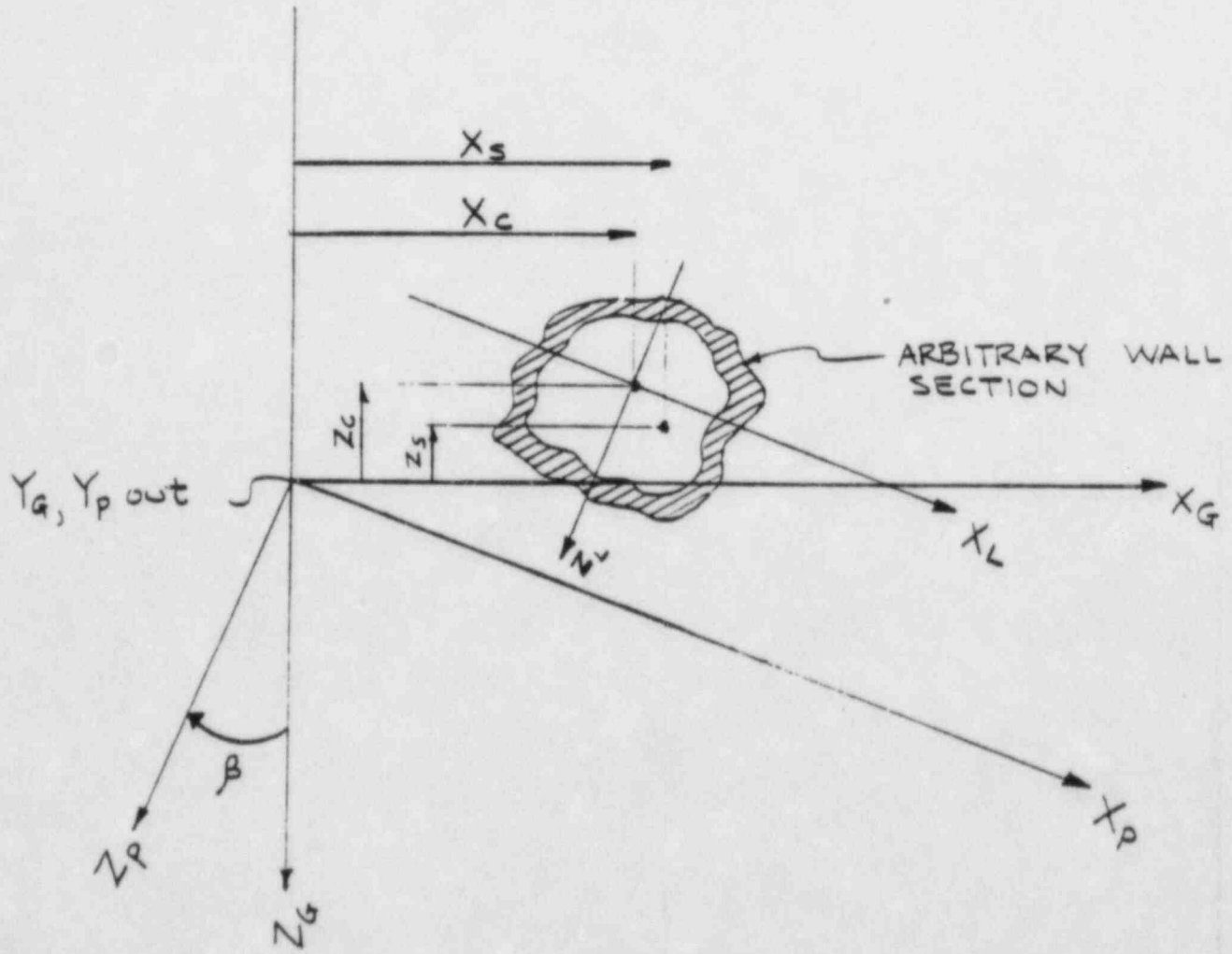

HORIZONTAL SECTION THROUGH WALL

X_s, Z_s = COOR. OF SHEAR CENTER OF WALL SECTION

X_c, Z_c = COOR. OF AREA CENTER OF WALL SECTION

* AS DEFINED BY RIG4, SEE FIGURE 2

EXAMPLE PROBLEM:

- AREA PROPERTIES OF WALL SECTION (ARBITRARY) ABOUT LOCAL PRINCIPAL AXIS

$A_{Y_L} = 6535.4 \text{ FT}^2$ $A_{X_L} = 3234 \text{ FT}^2$

$A_{Z_L} = 3723.7 \text{ FT}^2$

$I_{X_L} = 35015000 \text{ FT}^4$ $I_{Y_L} = 64200400 \text{ FT}^4$

$I_{Z_L} = 59953000 \text{ FT}^4$

- COOR, OF CENTER OF RIGIDITY IN GLOBAL AXIS SYSTEM

SHEAR CENTER: $X_S = 21.22 \text{ FT}$ $Z_S = -3.04 \text{ FT}$

AREA CENTER: $X_C = 19.68 \text{ FT}$ $Z_C = -5.61 \text{ FT}$

- COOR. OF CENTER OF MASS IN GLOBAL AXIS SYSTEM

MASS CENTER OF THE LOWER FLOOR:

$X_1 = 13.7 \text{ FT}$ $Y_1 = -0.5 \text{ FT}$ $Z_1 = -1.14 \text{ FT}$

MASS CENTER OF THE UPPER FLOOR:

$X_2 = 8.21 \text{ FT}$ $Y_2 = 28.5 \text{ FT}$ $Z_2 = -3.92 \text{ FT}$

- ANGLE OF PRINCIPLE AXIS:

$-\beta = -0.36 \text{ radians} = -20.62648^\circ$

$E = 432000 \text{ KSF}$

$G = 185100 \text{ KSF}$

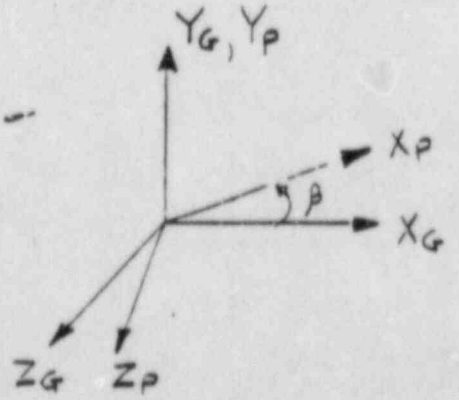

1. STRUDL RIGID MODEL:

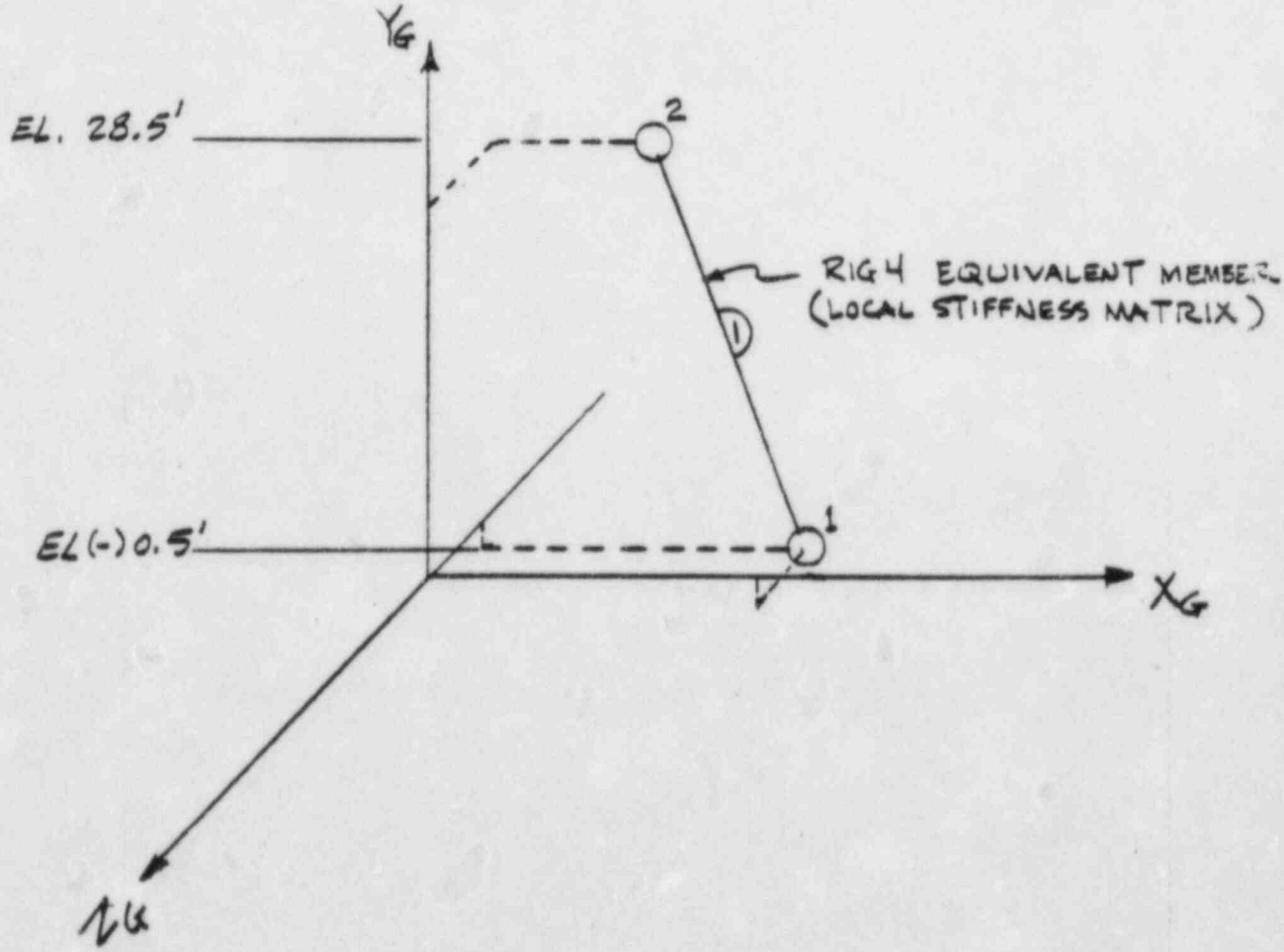

FIGURE 6

2. STRUDL FRAME MODEL:

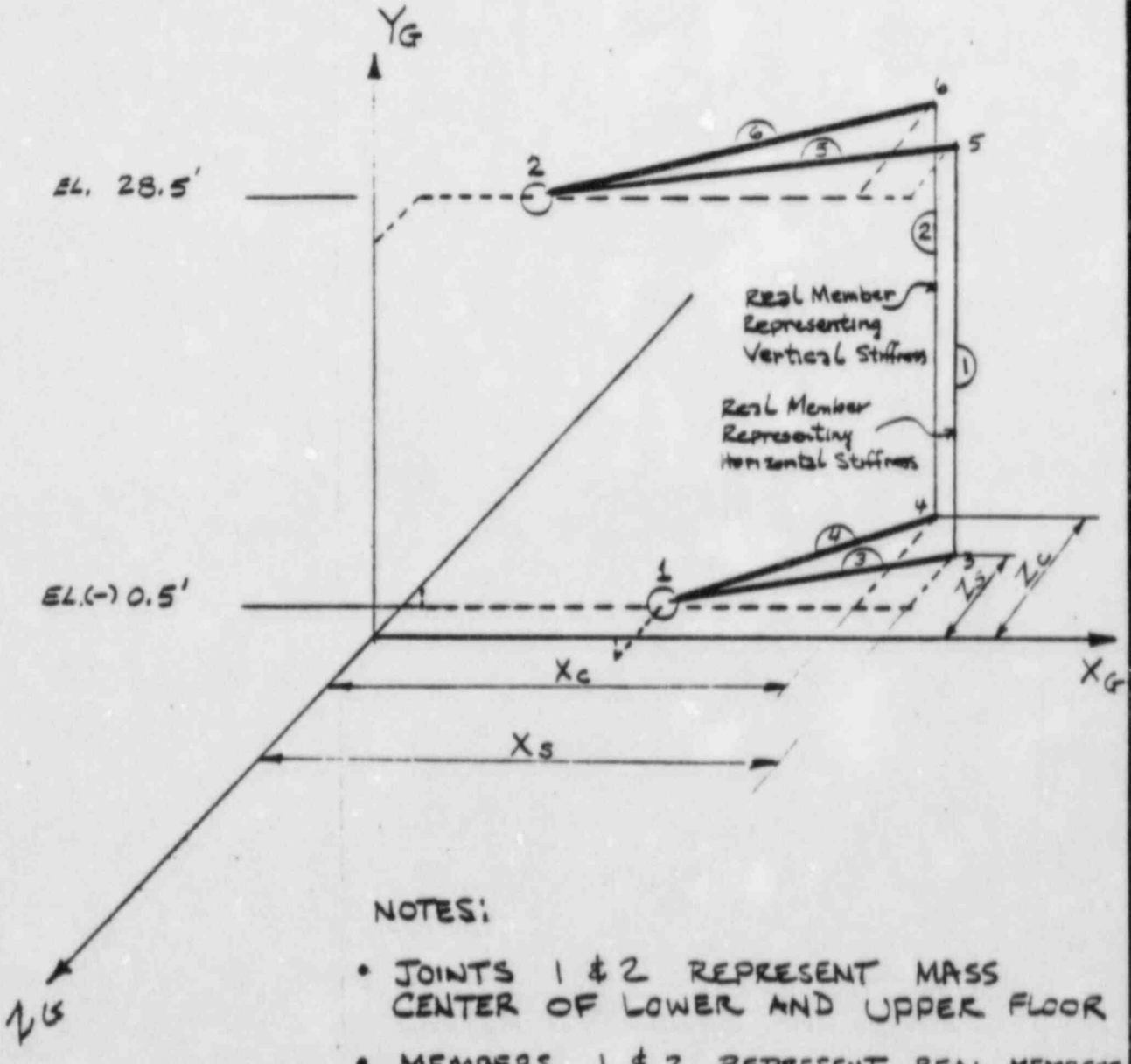

NOTES:

- JOINTS 1 & 2 REPRESENT MASS CENTER OF LOWER AND UPPER FLOOR
- MEMBERS 1 & 2 REPRESENT REAL MEMBERS
- MEMBERS 3 THRU 6 REPRESENT RIGID MEMBERS

FIGURE 7

TABLE 2

RESULTING GLOBAL STIFFNESS MATRIX (K_{AA})

1. FROM STRUDL RIG 4 MODEL

	1	2	3	4	5	6
1	1.749×10^{9}	-2.996×10^{4}	-8.473×10^{7}	1.474×10^{10}	3.170×10^{10}	3.044×10^{11}
2	-2.996×10^{4}	8.113×10^{9}	-1.492×10^{4}	1.645×10^{11}	-2.085×10^{6}	1.117×10^{13}
3	-8.473×10^{7}	-1.492×10^{4}	1.942×10^{9}	-3.38×10^{11}	-3.041×10^{11}	-1.474×10^{10}
4	1.474×10^{10}	1.645×10^{11}	-3.380×10^{11}	6.875×10^{14}	5.290×10^{13}	-1.444×10^{15}
5	3.170×10^{10}	-2.085×10^{6}	-3.041×10^{11}	5.290×10^{13}	4.965×10^{15}	5.508×10^{12}
6	3.044×10^{11}	1.117×10^{12}	-1.474×10^{10}	-1.444×10^{15}	5.508×10^{12}	1.037×10^{16}

2. FROM STRUDL FRAME MODEL

	1	2	3	4	5	6
1	1.749×10^{9}	0.0	-8.471×10^{7}	1.474×10^{10}	3.170×10^{10}	3.044×10^{11}
2	0.0	8.114×10^{9}	0.0	1.645×10^{11}	0.0	1.117×10^{12}
3	-8.471×10^{7}	0.0	1.942×10^{9}	-3.38×10^{11}	-3.041×10^{11}	-1.474×10^{10}
4	1.474×10^{10}	1.645×10^{11}	-3.380×10^{11}	6.874×10^{15}	5.292×10^{13}	-1.444×10^{15}
5	3.170×10^{10}	0.0	-3.041×10^{11}	5.292×10^{13}	4.965×10^{15}	5.515×10^{12}
6	3.044×10^{11}	1.117×10^{12}	-1.474×10^{10}	-1.444×10^{15}	5.515×10^{12}	1.037×10^{16}

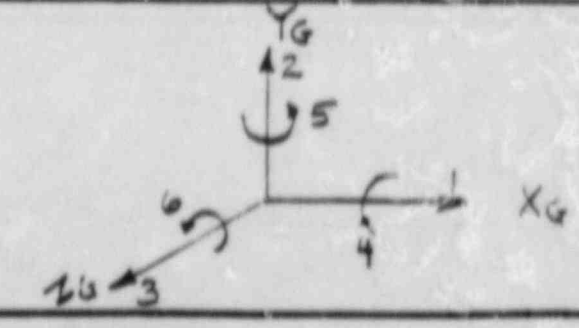

ITEM 15 With Respect to Ultimate Capacity of Containment

(i) Were elements that yielded prior to final yielding continuously checked to ensure that they were within acceptable ductility limits?

Response:

The Containment Structure's response due to an internal pressure was evaluated by the theory of thin shells utilizing the Axisymmetric Finite Element Method.

Figure 15-1 - Containment structure showing the critical Sections C_1 to C_5 and B_1 to B_3.

Figure 15-2 - Represents the model showing the centerline dimensions and nodes.

Figure 15-3 - Shows typical multilayered shell elements representing liner, concrete and reinforcement layers.

Figure 15-4 - Stress-strain curve for reinforcement and liner.
and 15-5

The ultimate pressure capacity of the containment is said to be achieved when all the layered elements across the section achieve a strain value corresponding to the elasto/plastic range. Since all the layered elements are connected by a single node, the hoop strain developed in the elements due to displacement of the node is constant across the section.

With constant strain across the section, the pseudo-nonlinear method as described in Section 3.2.3 of the Containment Failure Modes Report predicts the point of a general state of yield at a strain of approximately 0.005, well within the ductile range of the liner and reinforcing steel material (see figures 15-4, 15-5).

The attached Table 15-1 describes the event of responses at each section for various internal pressures.

ITEM 15 With Respect to Ultimate Capacity of Containment

(ii) Provide justification to indicate why the calculated ultimate pressure is the median of the probability distribution.

Response:

The failure pressure for each critical mode of failure of the containment is expressed as a probability distribution rather than a single point estimate (calculated). The variabilities (B) associated with the estimated nominal failure pressure are due to the Uncertainty and Randomness of the applicable parameters.

The significant variables that contribute to the uncertainty and randomness of the estimated failure pressure were as follows:

a) Material property variation (Randomness)

b) Construction variation (Randomness)

c) Analysis method employed (Uncertainty)

A single point estimate of the failure pressure was calculated by using average values for these variables as discussed in depth in Section 8 of the Containment Failure Modes Report. Due to insufficient and unavailable data for some of these variables as well as the limitations of the analysis it was a sumed through reasonable judgment that the calculated estimated failure pressures best represented the average value corresponding to a 50 percent probability of failure. Then for each established failure mode the total coefficient of variation and the standard deviation of the containment mean failure pressure was determined as shown in Table 15-2.

The resulting probability distribution, combining all the significant modes of failure, is presented in Figure 15-6. This cumulative distribution curve (Weibull distribution) represents the net conditional containment failure probability yielding a 5th, 50th, and 95th percentile failure pressure as indicated.

ITEM 15 With Respect to Ultimate Capacity of Containment

(iii) Review the basic shell/mat junction and demonstrate that compressive failure modes were adequately considered.

Item resolved pending the review of report and additional information. The Applicant will provide the additional information.

Response:

From the results of the finite element analysis, the axial force and bending moment as a function of internal pressure were determined for Sections B_1 and C_1, at the cylinder wall mat junction of the containment (see Figure 15-1). These sections were then evaluated for the axial forces and bending moments. The resulting liner, reinforcement, and concrete stresses and strains are presented in Tables 15-3 and 15-4. It is evident from a review of these tables that total yielding of all reinforcement occurs before a max concrete strain of 0.003 is achieved for both sections thus demonstrating that full capacity of the section is achieved prior to any compressive failure of the concrete.

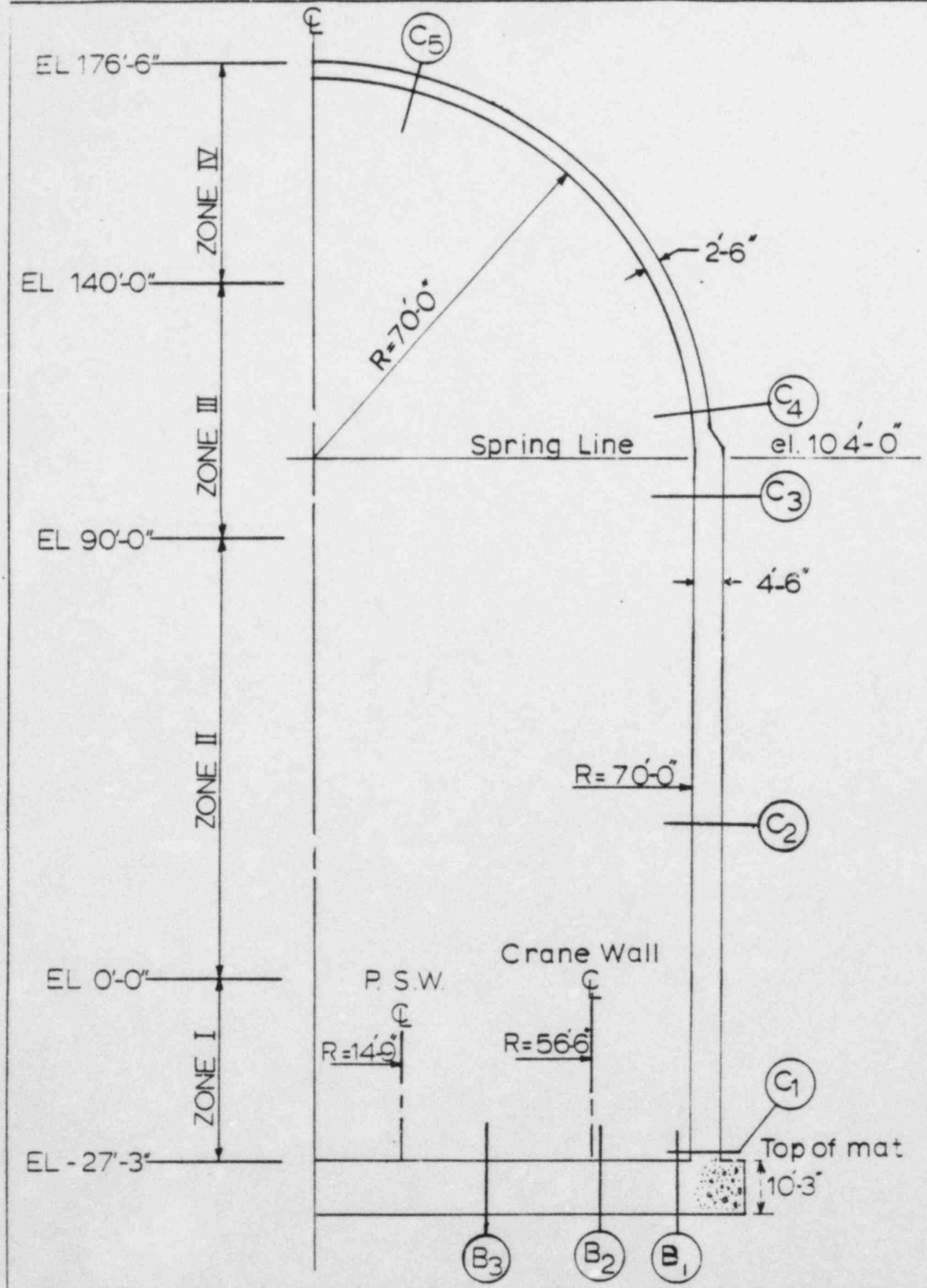

TITLE

CONTAINMENT SHELL AND MAT
CRITICAL SECTIONS

FIGURE 15-1

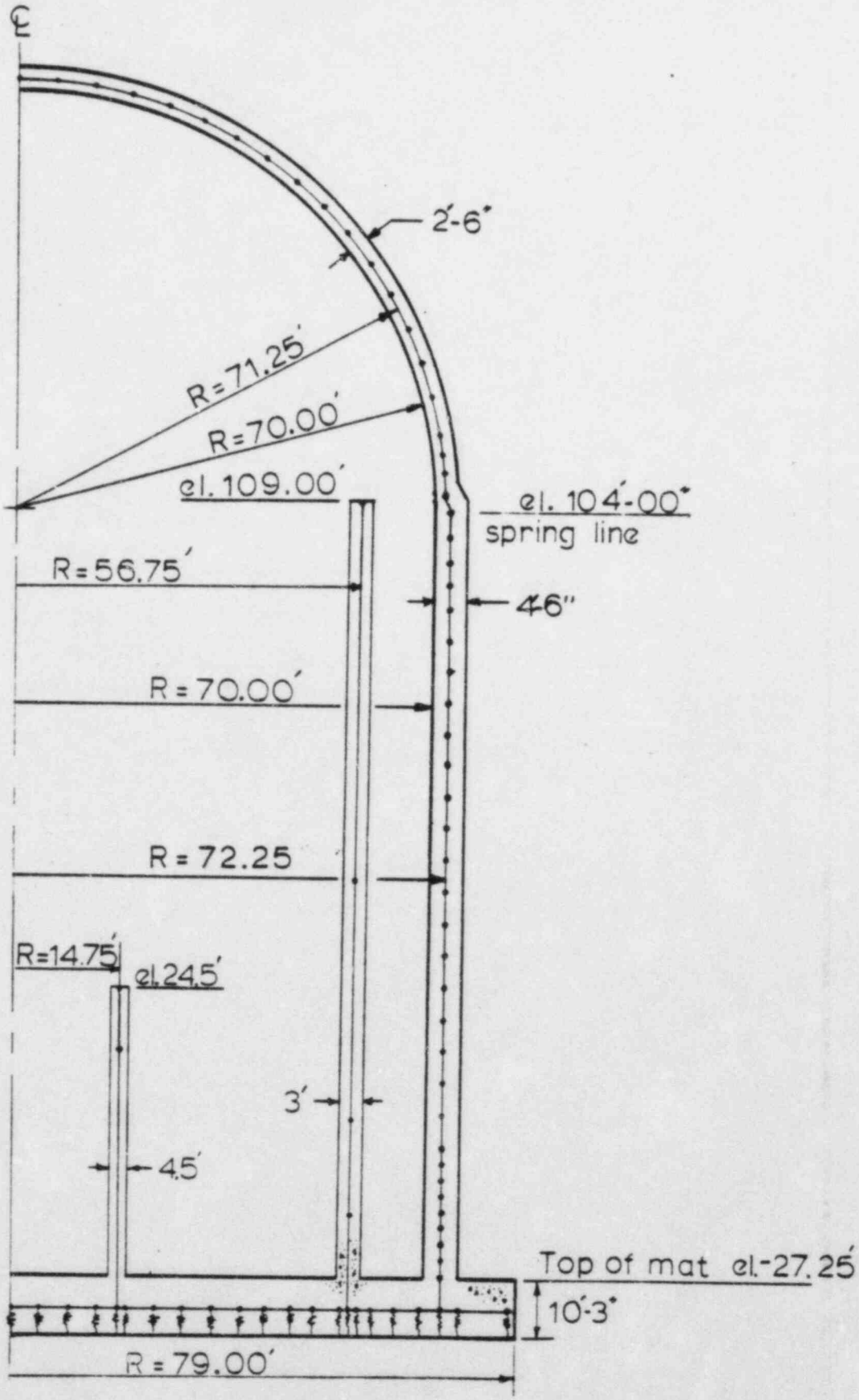

TITLE	FIGURE 15-2
CONTAINMENT STRUCTURE AXISYMMETRIC MODEL	

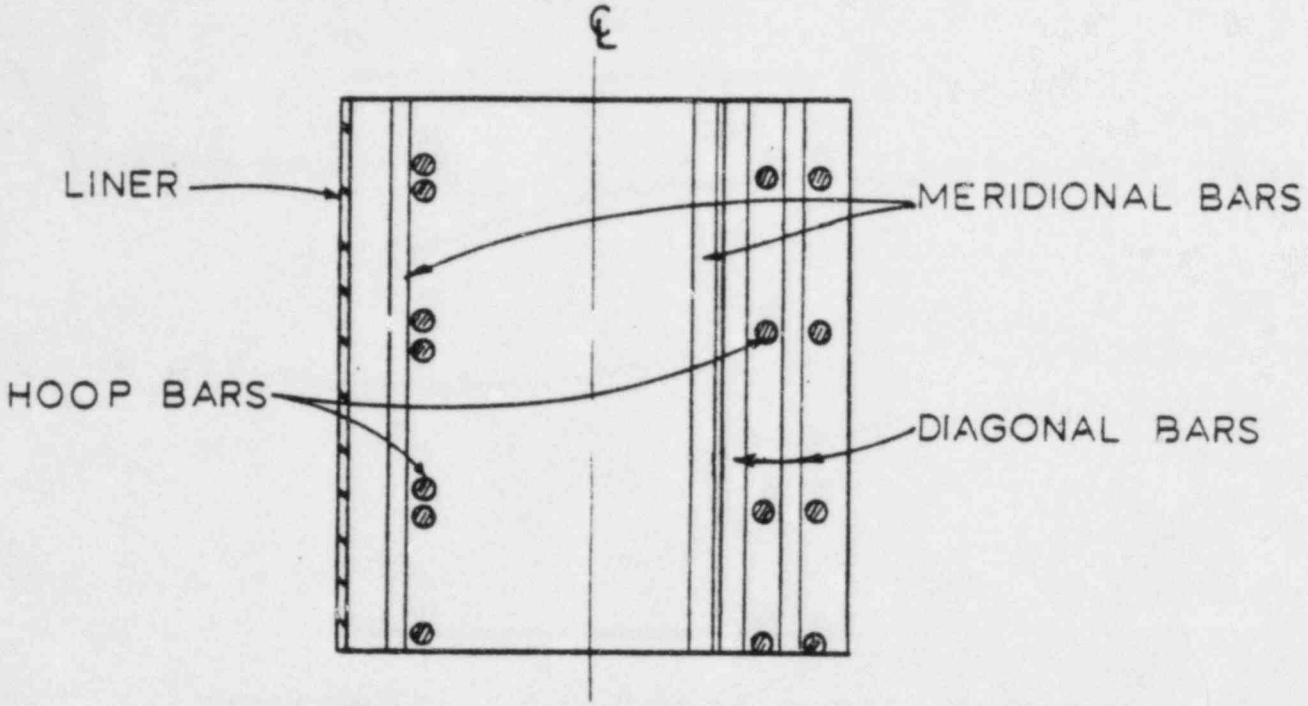

REINFORCED CONCRETE SHELL ELEMENT

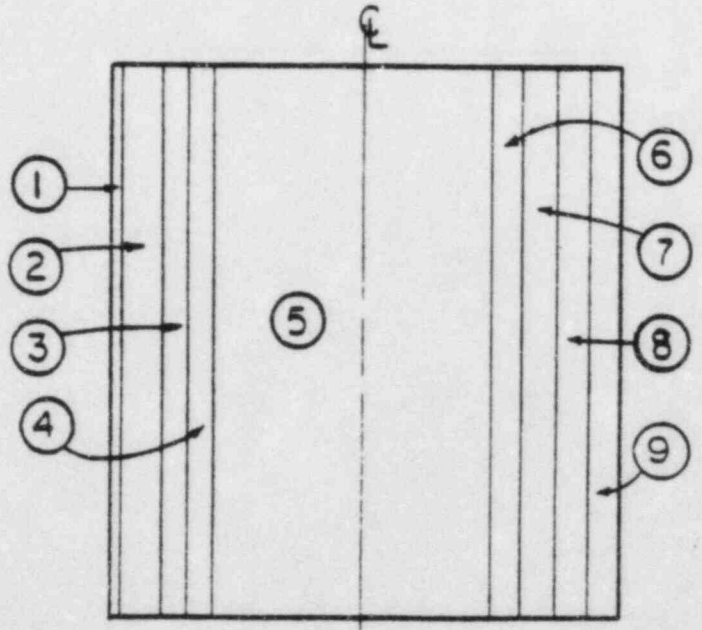

concrete layers: 2,5, 9

merid. steel layers: 3,6

hoop steel layers: 4,8

diagonal steel layer 7

liner layer 1

EQUIVALENT LAYERED ELEMENT

TITLE	FIGURE 15-3
SHELL ELEMENTS	

NOTE: TYPICAL RELATIONSHIP FOR ALL REINFORCING BARS, RELATIONSHIP SHOWN FOR No 18 BARS

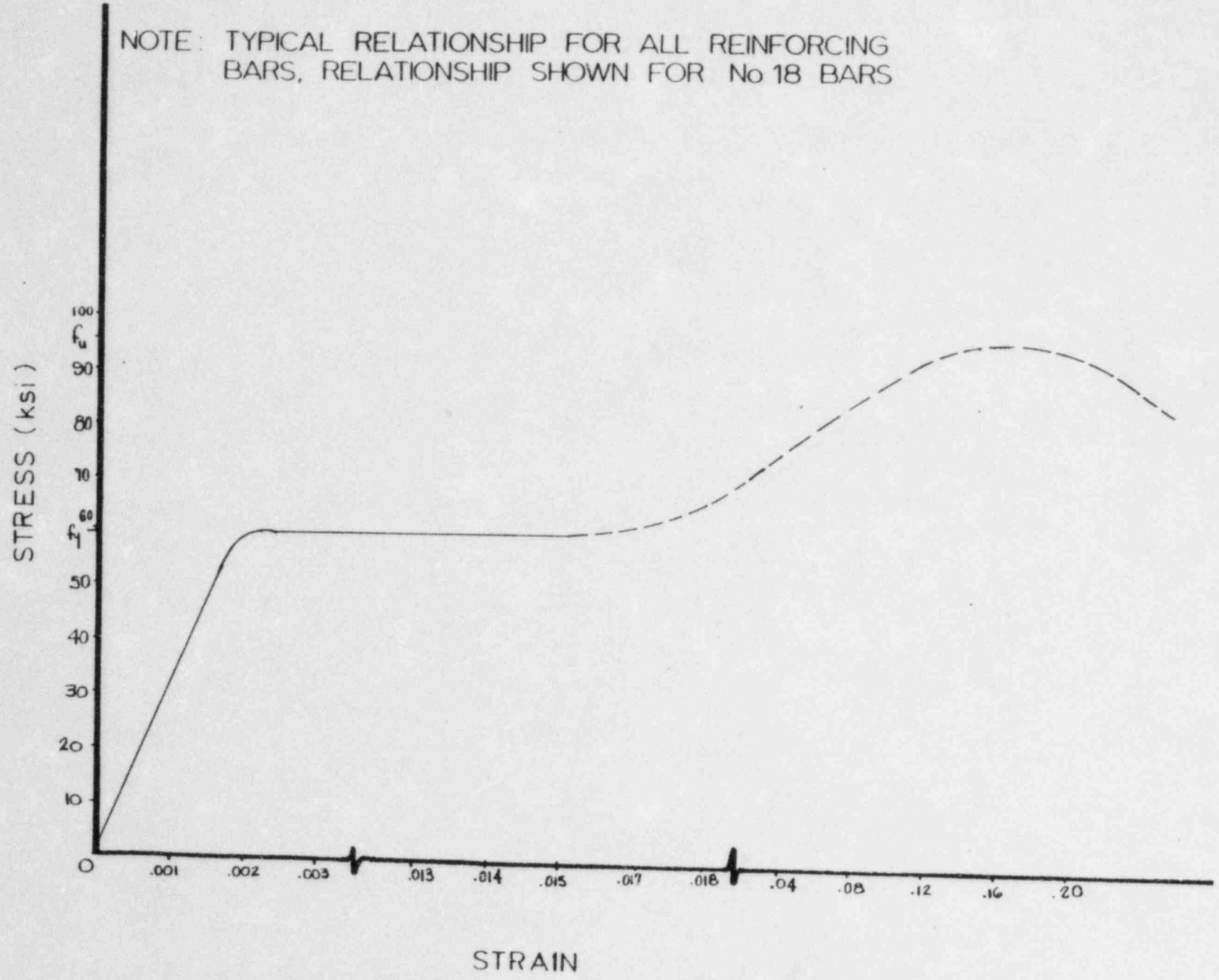

TITLE

STRESS-STRAIN CURVE FOR REINFORCEMENT

FIGURE 15-4

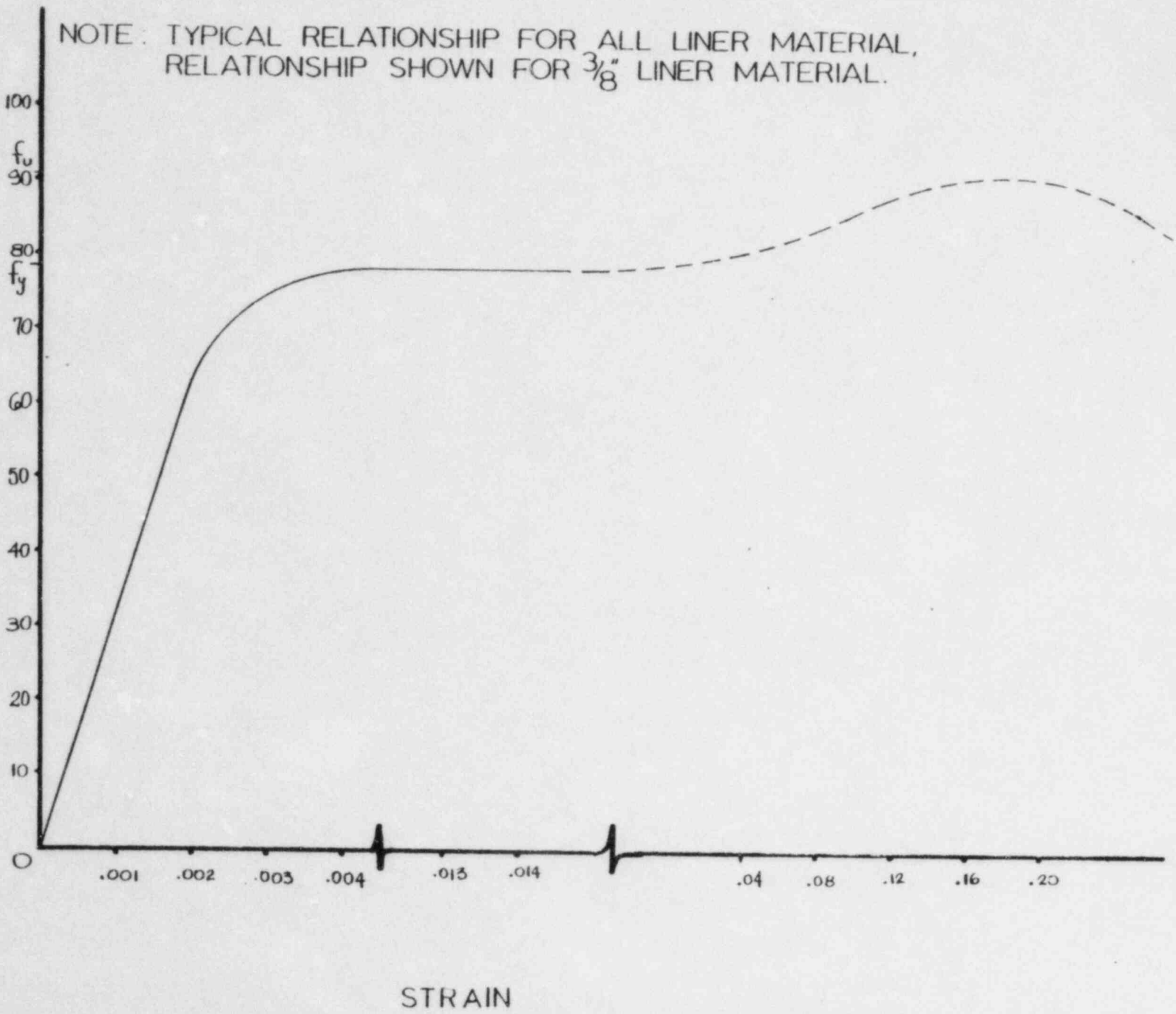

TITLE

STRESS-STRAIN CURVE FOR LINER

FIGURE 15-5

STONE & WEBSTER ENGINEERING CORPORATION

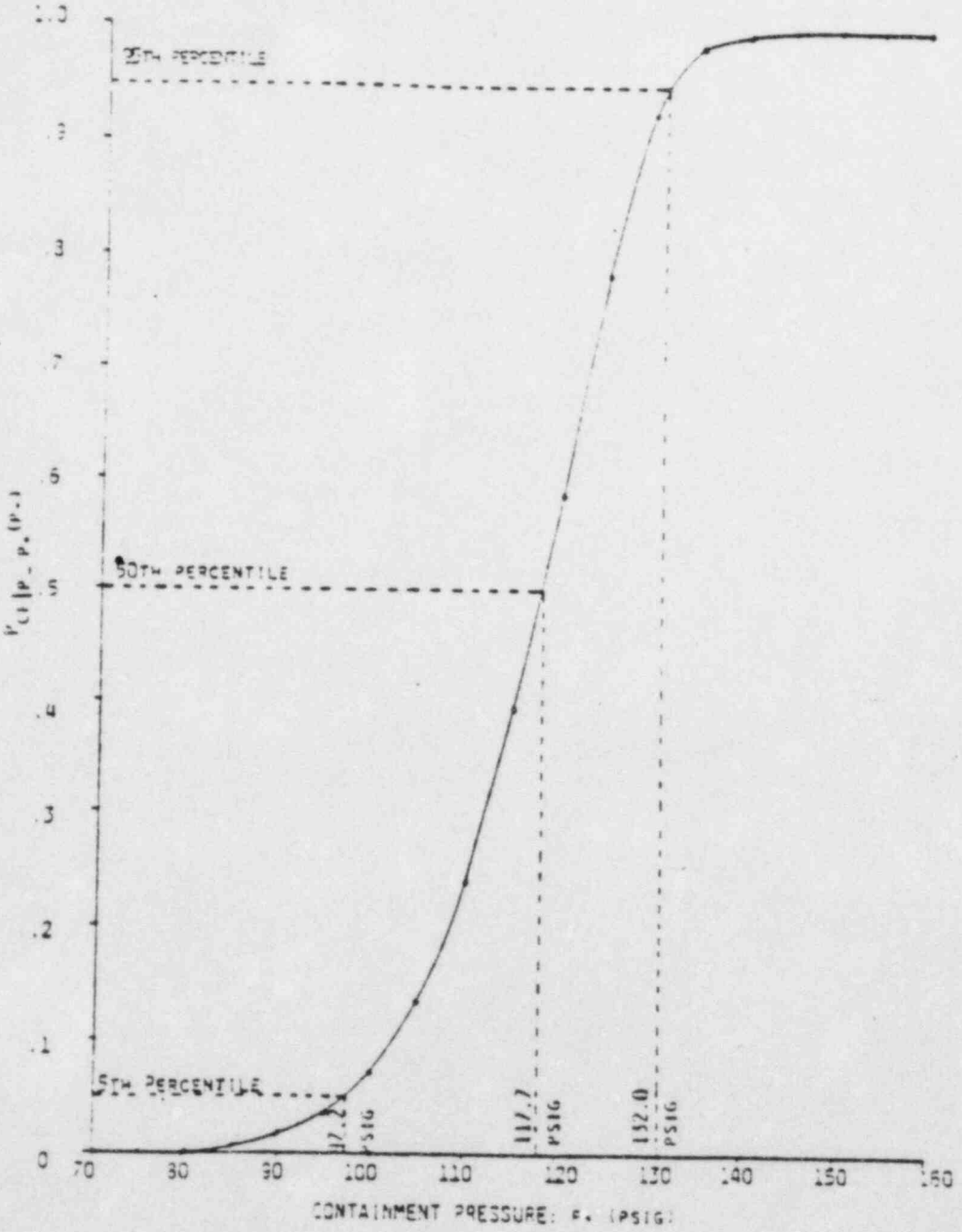
95TH PERCENTILE
50TH PERCENTILE
5TH PERCENTILE
1.0
.9
.8
.7
.6
.5
.4
.3
.2
.1
0
70
80
90
100
110
120
130
140
150
160
117.7 PSIG
132.0 PSIG
CONTAINMENT PRESSURE: P_c (PSIG)

Figure 15-6

TABLE 15-1

RESPONSE STAGES OF CYLINDER AND DOME

Pressure (psig)	Zone	Containment Response
100	II III IV	All zones in elastic range
104	II	Elastic range
	III	Liner yields in hoop directions at Section C_4
	IV	Elastic range
124	II	Hoop reinforcement yields at Section C_2
	III	Liner continues yielding increasing toward apex of dome
	IV	Elastic range
128	II	Liner yields in hoop direction at C_2 Hoop reinforcement continues yielding increasing in Zone II General state of yield at C_2 in hoop direction
	III	Liner continues yielding increasing toward apex of dome
	IV	Liner begins to yield in hoop direction at lower portion of zone
131	II	General state of yield in hoop direction entire zone Hoop strain reaches 0.005 limit at Section C_2
	III	Liner continues yielding
	IV	Liner continues to yield increasing toward apex of dome
132	II	Liner and hoop reinforcement continue straining
	III	Hoop reinforcement yields at Section C_4 Liner continues yielding General state of yield in hoop direction at Section C_4
	IV	Liner continues to yield increasing toward apex of dome

TABLE 15-1 (Cont)

133	II	Liner and hoop reinforcement continue straining
	III	General state of yield in hoop direction Hoop strain reaches 0.005 at Section C_4
	IV	Liner continues yielding

TABLE 15-2

MEAN FAILURE PRESSURES AND TOTAL VARIATIONS

Zone	Mean Failure Pressure (psig)	Total Coefficient of Variation (β)	Standard Deviation (psig)	Mean Failure Pressure (psig) +One Standard Deviation	Mean Failure Pressure (psig) -One Standard Deviation
I @ C_1	140	0.094	±13.2	153.0	127.0
II @ C_2	128	0.073	± 9.3	137.0	119.0
III @ C_4	132	0.079	±10.4	142.0	122.0
IV @ C_5	≥145	0.082	±11.9	157.0	133.0
Containment Mat					
Section B_1	155	+0.090 -0.084	+14.0 -13.0	169.0	142.0
Section B_4	140	+0.096 -0.089	+13.4 -12.5	153.0	128.0
Piping Penetrations					
Main Steam	128	0.110	14.1	142.0	114.0
Feedwater	131	0.108	14.1	145.0	117.0

TABLE 15-3

CONTAINMENT MAT @ SECTION B_1
STRESSES AND STRAINS

Pressure (psi)	Stress (ksi) Liner	Reinforcement**	Concrete*	Strain Liner	Reinforcement**	Concrete*
100	37.0	33.1	-1.3	0.00124	0.00110	0.00030
115	43.6	38.9	-1.5	0.00145	0.00130	0.00036
121.5	46.5	41.5	-1.6	0.00155	0.00139	0.00039
130	50.3	44.9	-1.8	0.00168	0.00150	0.00042
135	52.5	46.9	-1.9	0.00175	0.00156	0.00044
140	54.7	48.9	-1.94	0.00182	0.00163	0.00046
145	56.5	51.0	-2.0	0.00190	0.00170	0.00048
150	56.5	53.7	-2.1	0.00201	0.00179	0.00050
155	56.5	56.5	-3.4	0.00589	0.00513	0.00083

*Max. values tabulated
**Average value for reinforcement tabulated

TABLE 15-4
CONTAINMENT CYLINDER @ SECTION C_1
STRESSES AND STRAINS

Pressure (psi)	Stress (ksi) Liner	Reinforcement**	Concrete*	Strain Liner	Reinforcement**	Concrete*
100	50.6	37.4	-3.6	0.00169	0.00125	0.00090
115	56.5	44.0	-4.0	0.00198	0.00147	0.00105
121.5	56.5	47.8	-4.2	0.00215	0.00159	0.00113
130	56.5	52.98	-4.5	0.00250	0.00186	0.00127
135	56.5	56.1	-4.7	0.00281	0.00210	0.00139
140	56.5	56.5	-5.0	0.00714	0.00547	0.00269

*Max. values tabulated
**Average value for reinforcement tabulated